ELSEVIER

Journal of Molecular Catalysis A: Chemical 167 (2001) 199–206

JOURNAL OF MOLECULAR CATALYSIS A: CHEMICAL

www.elsevier.com/locate/molcata

The behavior of vapor deposited Co layers on MoO_3 surfaces at 90 and 300 K

L. Viscido [a], M. Voß [b], D. Borgmann [b], J.M. Heras [a,*]

[a] *Institut of Physical Chemistry (INIFTA), University of La Plata, CONICET, CICPBA, C.C. 16, Suc. 4, 1900 La Plata, Argentina*
[b] *Institute of Physical and Theoretical Chemistry, University of Erlangen-Nüremberg, Egerlandstr. 3, D-91058 Erlangen, Germany*

Received 4 April 2000

Abstract

The interaction of evaporated Co atoms with polycrystalline MoO_3 surfaces at 90 and 300 K was studied by means of X-ray photoelectron spectroscopy (XPS). The MoO_3 samples (∼300 nm thick) were prepared by oxidation of a Mo 99.9% foil at 800 K in a flow of O_2 at ∼1 bar. X-ray diffraction spectra indicated that only MoO_3 was obtained. From the very beginning of the deposition the Co 2p spectra showed the presence of Co^{2+} species even at 90 K, while at higher coverages the Co^0 increased steadily. Simultaneously, a shoulder in the Mo 3d spectra indicated the formation of Mo^{4+} and Mo^{5+} species. The following annealing up to 800 K revealed that above 500 K, the Co^0 species also begin to be oxidized. A careful deconvolution procedure of the experimental signal indicates that part of the Mo^{4+} and Mo^{5+} species transformed slowly into Mo^{6+}. At both deposition temperatures, after a thorough annealing at 800 K the main product obtained was a non-stoichiometric Co-molybdate, as data of the binding energies of the Mo 3d peaks of this compound suggest.

Keywords: Cobalt overlayers oxidation; Molybdenum oxides reduction; AES; XPS

1. Introduction

Molybdenum trioxide is an active and selective catalyst for the partial oxidation of alcohols and hydrocarbons [1–3]. In addition, MoO_3 based catalysts are widely used for methane oxidation [4–9]. The surface properties of Mo oxides have been a recurring research object for various decades [10]. MoO_3 is known to exhibit an intrinsic variability in the oxygen content and a whole series of ordered oxygen defective structures is known to exist in the range between MoO_3 and MoO_2. Moreover, defect structures may be produced on MoO_3 under mechanical stress [11]. Undoubtedly, all of them modify the electronic properties of the material. In fact, the relationship between the different crystal planes of MoO_3 and their contribution to catalyst performance are very important for identification of active sites in the catalyst [12,13]. Moreover, the nature of the support and its surface morphology influence the MoO_3 dispersion [14–16] which in turn, influences the behavior of adsorbed particles (i.e. Co atoms). Cobalt/molybdenum catalysts also show versatile catalytic properties and are widely used in crude hydrodesulphurization processes where activity derives from a reduced state of Mo^{6+}. Actually, besides Mo^{6+} and Mo^{4+}, substantial amounts of Mo^{5+} have been detected with XPS upon activation of a cobalt–molybdena–alumina catalyst by reduction [17]. Many papers also refer to surface oxidation reactions of cobalt and molybdenum, studied through

* Corresponding author. Tel.: +54-221-425-7430, Ext. 124; fax: +54-221-425-4642.
E-mail address: surfaces@inifta.unlp.edu.ar (J.M. Heras).

1381-1169/01/$ – see front matter
PII: S1381-1169(00)00507-0

XPS [18,19]. In the last decade, our groups have investigated Co and Mo surfaces focusing the interest in: the interaction of oxygen and water with Co single crystals [20–24]; the activation and deactivation of cobalt catalysts in the hydrogenation of CO_2 [25–28]; the interaction of oxygen with thin Co films supported on silica [29] or on polycrystalline Mo foils [30] and the interaction of CO_2 with polycrystalline Mo [31]. A first overview on the reaction of deposited Co with MoO_3 surfaces is given in [32].

The present paper deals with the interaction of vapor deposited Co atoms with a thin layer of MoO_3 grown on a polycrystalline Mo support, in order to eliminate the influence of the more conventional alumina support. Reduction to Mo^{5+}, Mo^{4+} and finally, upon annealing at 800 K, re-oxidation to Mo^{6+} mainly in a molybdate matrix are the principal results discussed. This paper is part of a more comprehensive research program in order to develop a Mo/Co catalyst model.

2. Experimental

The XPS studies were performed in an all-metal UHV system (ESCALAB 200, VG Scientific working with constant pass energy mode at 20 eV), also equipped with a quadruple mass spectrometer and a Co filament evaporation source. An Al Kα anode X-ray source (excitation energy of 1486.6 eV) was used. The energy scale was calibrated to the binding energy (BE) of Au $4f_{7/2} = 83.8$ eV. The MoO_3 layers with thicknesses ranging between 300–400 nm were produced on thin Mo foils (Goodfellow Metals, 99.9% pure) in a continuous flow reactor at 800 K and ∼1 bar of oxygen (99.9% pure) for ∼10 h. These thicknesses were selected to ensure (i) no interface influence on the spectra (the interface is not visible to XPS), and (ii) no sample charging effects. The preparation procedure was optimized by X-ray diffraction analysis, which shows that in all the samples only MoO_3 was formed. Small amounts of carbon contamination detected by XPS could be removed by heating up to ∼900 K under UHV conditions. Bombardment with Ar or O_2 ions causes a reduction of the MoO_3 surface [30]. Co was stepwise deposited onto the clean MoO_3 surface at 90 and 300 K by sublimation of a Co wire (Goodfellows Metals, 99.99% pure) mounted in a home made evaporator with a cold water shroud. With this filament system, evaporation rates of ∼0.05 monolayers per minute are routinely achieved.

The Mo 3d, C 1s, O 1s, Co 2p signals were monitored, sometimes together with the valence band region and the O_{KLL} Auger region. After satellite substraction, a Shirley background correction was applied to all spectra. In order to assign the contribution of the different oxide states, the peaks were fitted using commercial *software* with 30% Lorentzian lines and a constant spin-orbit-splitting (3.14 eV for the Mo $3d_{5/2}$ and $3d_{3/2}$ signals; 15, 15.5 and 16 eV for the Co $2p_{3/2}$ and $2p_{1/2}$ in the Co^0, Co^{2+} signals and shake-up satellites, respectively). Additionally, the fitting algorithm assumed a constant intensity ratio of the doublets based in the theoretical ratios. FWHM were set for each type of signal: ∼1.8 eV for Mo 3d (1.6–1.9 eV, depending on the oxidation state); 2.5, 4 and 5 eV for Co 2p in Co^0, Co^{2+} and shake-up satellites, respectively. The estimated accuracy of the fitted binding energies was ±0.1 eV.

3. Results and discussion

In Fig. 1, the Mo 3d XP spectra taken after some Co evaporation steps are given. Deposition was performed at 90 (part a) and 300 K (part b). The topmost curve corresponding to clean MoO_3 (part a) could only be fitted at the low energy side of the spectrum if, besides the signals of Mo^{6+} $3d_{5/2}$ (232.7 eV) and Mo^{6+} $3d_{3/2}$ (235.8 eV), a small signal assigned to the Mo^{5+} doublet (231.1–234.2 eV) was taken into account. In some samples, when applying the fit routine to the Mo 3d signals, an additional doublet corresponding to Mo^{4+} (229.6–232.8 eV) also had to be considered, because of a clear "bump" observed at BE ∼229 eV (absent in Fig. 1a). A possible explanation for the appearence of Mo oxidation states lower than 6+ on the freshly prepared MoO_3 is the reduction by the small carbon contamination detected in the as-mounted samples. The possible amounts of CO formed and desorbed were not detected by mass spectrometry. Comparing parts a and b of Fig. 1, it is clear that with increasing amount of deposited Co, a shoulder in the low energy side of the Mo 3d spectra grows up indicating the formation of Mo^{4+} and possibly of Mo^{5+}. The reduction of Mo^{6+} proceeds more rapidly at 300 K than at 90 K (compare the

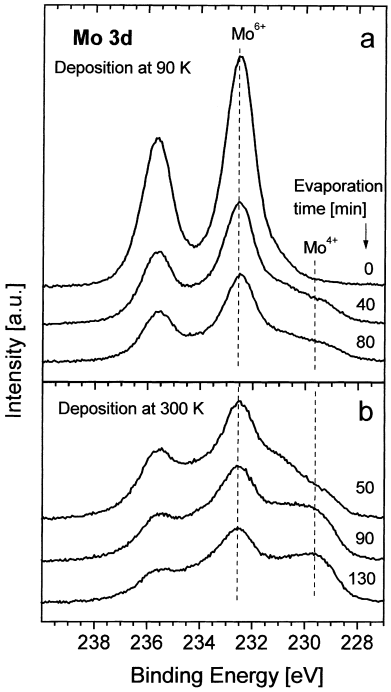

Fig. 1. Mo 3d XP spectra after deposition of Co at 90 (part a) and 300 K (part b). Details in the text.

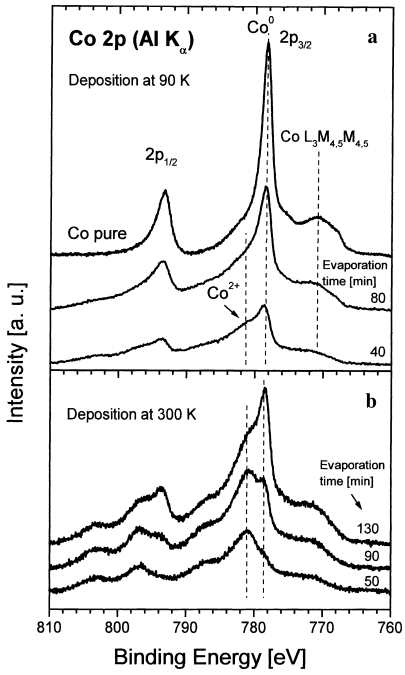

Fig. 2. Co 2p XP spectra as deposition proceeds, taken at 90 (part a) and 300 K (part b). Details in the text.

curve labeled 80 min of Fig. 1a with that of 90 min in Fig. 1b).

After 130 min evaporation at 300 K, a hcp-equivalent cobalt layer thickness of ∼5 monolayers can be estimated from the attenuation of the Mo 3d signal. Due to the strong interaction between Co and MoO_3 lateral diffusion seems unlikely at 90 K, while incorporation in the MoO_3 matrix of part of the Co atoms can be proposed instead especially at 300 K. This incorporation proceeds via oxidation to Co^{2+} as explained in the following.

The BE of Mo^{6+} and Mo^{5+} obtained after the fitting procedure correlate very well with data from the literature [19,33]. However, the Mo^{4+} signal shows small deviations of 0.1 eV [33] and 0.4 eV [19], respectively.

Fig. 2 shows the Co 2p region of the spectra, taken at 90 (part a) and 300 K (part b) after different deposition times. The shoulder at the low energy side (773.8 eV) is assigned to the Co $L_3M_{45}M_{45}$ Auger signal (Al Kα radiation!). As deposition proceeds, the Co 2p peaks point to an increasing amount of Co^{2+} at a BE of 781.1 eV (obtained after deconvolution), especially at 300 K. Typical of the formation of Co^{2+} are the shake-up satellites at the high energy side of the spectra [34]. With increasing Co deposition time at 300 K (Fig. 2b), an increase in intensity and a shift of the signal towards 780.7 eV are observed. However, when deposition is performed at 90 K (Fig. 2a) the characteristic spectrum of Co metal dominates. This is represented by the upper curve, taken in the same apparatus under similar conditions on a Co polycrystalline sheet, 99.999% pure. The small shift to higher BE after evaporation at 300 K (Fig. 2b) is attributed to an incorporation of Co^{2+} ions in the MoO_3 matrix. The comparison with reference data taken with the same spectrometer and those reported in the literature [34] shows that even after 130 min deposition at 300 K the Co^{2+} is still influenced by the MoO_3 matrix, since there remain deviations of the BE compared to that of CoO given in the literature (+0.7 and +0.6 eV compared to [35,19]). With increasing evaporation time at 300 K (Fig. 2b) the Co^0 signal at 778.4 eV can also be observed.

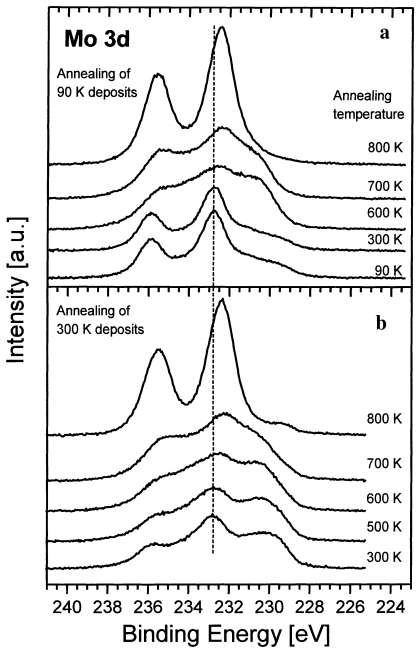

Fig. 3. Changes in the Mo 3d XP spectra after annealing. Deposits obtained at (a) 90 K; (b)300 K.

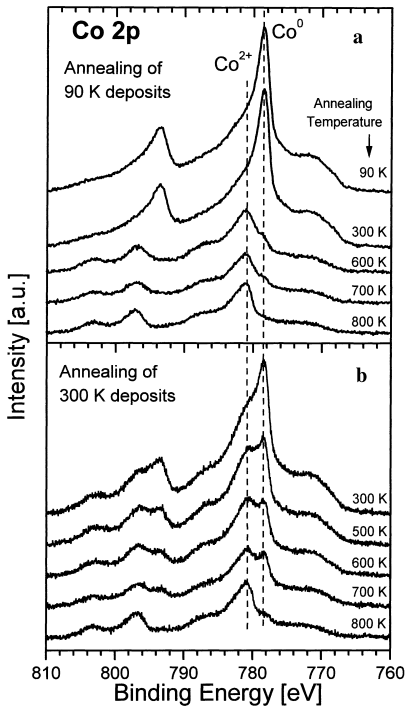

Fig. 4. Changes in the Co 2p XP spectra after annealing. Deposits obtained at (a) 90 K; (b)300 K.

Once the deposition procedure was over, the system was heated in steps up to 800 K maintaining the corresponding annealing temperature for 10 min. In each case, before taking XP spectra the sample was allowed to cool down to ∼300 K. Finally, a 2 h annealing at 800 K was performed. Fig. 3 shows the changes in the Mo 3d region for deposits at 90 and 300 K (parts a and b, respectively). At both deposition temperatures dramatic changes in the Mo 3d spectra occur above 500 K: at the end of the 800 K annealing a feature resembling that of Mo^{6+} 3d was re-established, but with a shift of 0.4 eV towards lower BE as compared to MoO_3 (see Figs. 1 and 3). A careful fitting procedure applied to these Mo 3d XP spectra yields a significant decrease of the Mo^{4+} and the Mo^{5+} signal intensities, while a good fit can be obtained only including two types of Mo^{6+} signals with the Mo $3d_{5/2}$ peaks at 232.7 and 232.3 eV. The first corresponds obviously to the MoO_3 matrix while the second can be assigned undoubtedly to a molybdate matrix [19]. [1] It should be stressed that a fit with only one doublet having the Mo $3d_{5/2}$ peak at ∼232.5 eV is always worse.

In the same way the Co 2p spectra for both deposition temperatures are shown in Fig. 4. This figure shows the change from mainly an intensity of Co^0 (topmost spectrum at both deposition temperatures) to a strong Co^{2+} intensity at 800 K. A shift of the Co^{2+} intensity from 780.7 to 781.2 eV after annealing at 500–600 K indicates a change in the ion environment of the probed layer as annealing proceeds. The deposits obtained at 90 K (Fig. 4a) clearly show that annealing between 300 and 600 K causes a considerable decrease in peak intensities. This can be explained by the incorporation of the surface Co^0 atoms into the bulk of MoO_3 as Co^{2+} ions.

Noteworthy, these Figs. show that between 600 and 700 K, a dramatic reorganization process takes place within the probed layer, which leads to the formation of a species assumed to be molybdate. Actually, the 0.4 eV shift of the Mo^{6+} signal to lower BE above 500 K can only be explained by the formation of a

[1] For these spectra we are thankful to A.R. González-Elipe of the Instituto de Ciencias de Materiales de Sevilla, Spain.

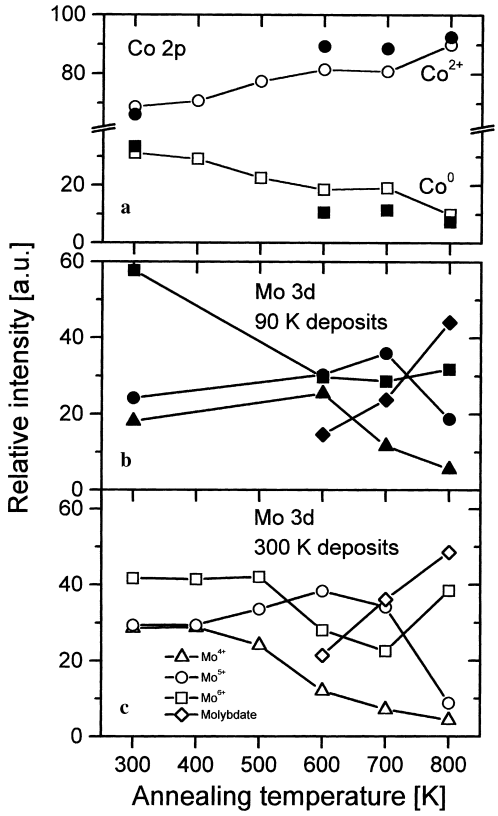

Fig. 5. Relative intensity of the different species contributing to the profiles of Co 2p (part a) and Mo 3d (parts b and c) during annealing. Note the dramatic changes above 600 K. Open symbols refer to 300 K deposits, filled symbols to 90 K deposits. In parts b and c, the symbol △ indicates Mo^{4+}; ○ Mo^{5+}; □ Mo^{6+} in MoO_3 and ◇ Mo^{6+} in molybdate.

Co molybdate. McIntyre et al. [19], on self prepared $CoMoO_4$, reported a Mo $3d_{5/2}$ BE of 232.2 eV which correlates very well with the present value of 232.3 eV. Moreover, the same value as McIntyre's was obtained in a 99.9% pure $CoMoO_4$ sample (All-Chemie Ltd., Mt. Pleasant, USA[1]).

Fig. 5 summarizes the contribution that each oxidation state makes to the Co 2p and Mo 3d profiles obtained by the above mentioned fitting procedure during annealing. This figure shows that besides the molybdate matrix, there remain in the probed thickness some Mo^{4+} and Mo^{5+} species embedded in a MoO_3 matrix. Comparing the Co $2p_{3/2}$ BE of the Co^{2+} species, the value in both molybdate samples is 780.8 eV, while in the present system after a thorough annealing at 800 K the value of 781.2 eV was obtained independently of deposition temperature. The small difference of 0.4 eV with respect to the value in $CoMoO_4$, possibly arises from the influence of matrix effects. These effects arise not only because of the remaining Mo^{4+} and Mo^{5+} species, which have "supplied" part of the necessary oxygen ions to oxidize the Co, but also from crystallinity degradation due to the displacement of the oxygen ions from the bulk of MoO_3. In fact, it is known that in group VIb transition metal oxides, and due to their usual defective structure [11] (e.g. edge linked metal–oxygen octahedra or tetrahedra in the case of MoO_3), there is a very rapid oxygen ion transport compared to the diffusion of oxygen atoms observed in the closed packed structure of the majority of the transition metal oxides [36]. In other words, when Co atoms incorporate as Co^{2+} there should be enough Mo^{4+} and Mo^{5+} species created in the bulk of the MoO_3 matrix *beyond the escape depth* of the Mo 3d electrons to account for all the necessary oxygen ions to form the molybdate in the outer probed volume. Actually, a somewhat oxygen defective structure should be expected.

Fig. 6 shows the valence band region in the case of Co deposition at 90 K. The first curve clearly shows the insulating behavior of the clean MoO_3. After 80 min deposition the Co layer confers metallic characteristics to the sample, which are practically lost after annealing at 800 K, when the molybdate is formed (lower curve).

Fig. 7 shows the X-ray excited oxygen KLL Auger spectra after differentiation to enhance the features. The feature at 521 eV kinetic energy associated with oxide compounds with an oxygen–metal bond of strong covalent character [37], is worth noticing. This characteristic fades out upon Co deposition and annealing at 800 K.

The O 1s XP spectra always show only one peak at 530.4 eV (Co_3O_4 has two O 1s peaks [34]), which develops a tail towards high binding energies upon Co deposition. This peak shape change can be assigned to low co-ordinated oxygen ions at the surface of the sample because of the Co^{2+} ions penetrating the MoO_3 matrix and causing a crystallographic disorder [34]. It has been reported that differences in the Madelung potential around the oxygen ion can be responsible for the tail at high BE in the O 1s photoemission spectra [38]. In fact, the O 1s peak can be deconvoluted

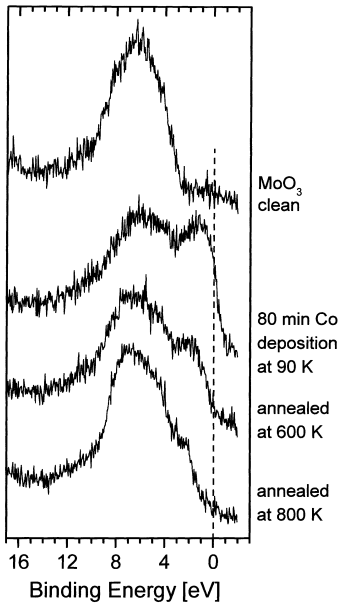

Fig. 6. Valence band XP spectra, recorded in the same spectrometer with Al Kα radiation. Details in the text.

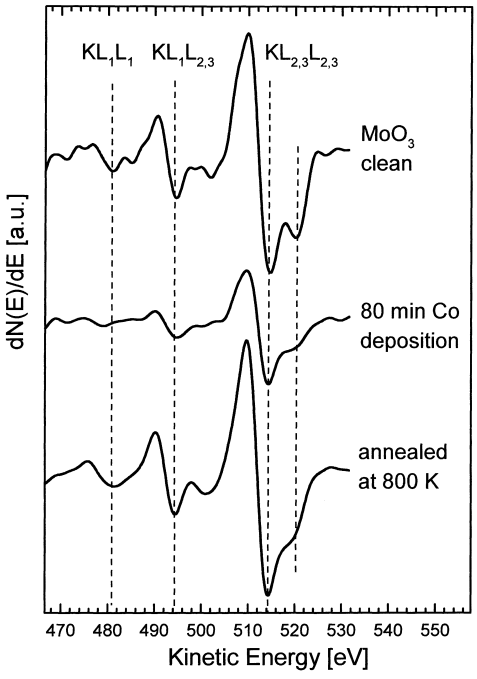

Fig. 7. Oxygen KLL Auger spectra shown in derivative form to enhance the feature at 521 eV. Details in the text.

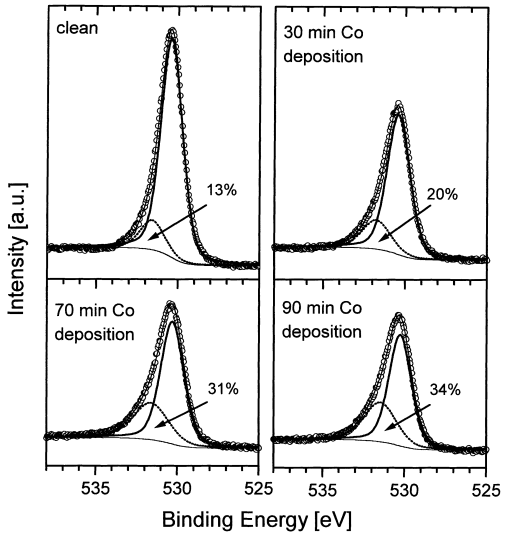

Fig. 8. Deconvolution of the O 1s XP spectra during Co deposition at 300 K. Open circles, experimental data; dotted curve, necessary component to account for the high BE tail.

into two peaks, one at 530.35 ± 0.05 eV, another at 531.6 ± 0.1 eV of very small intensity which increases its contribution as Co deposition proceeds (see Fig. 8, which is also an example of the fitting procedure). This contribution of ∼34% is dramatically reduced when the system was annealed for 10 min at 800 K, reaching values even below the one estimated in the clean MoO_3 surface. Noteworthy, this shape deformation is absent in $CoMoO_4$.[1] These facts clearly indicate that the shape of the high BE tail of the O 1s peak depends on the matrix order. Taking into account the complex MoO_3 crystal structure [39], with Mo–O bond lengths ranging from 167 to 233 pm, the matrix deformation caused by incorporation of the Co atoms as ions can be healed up supplying the energy represented by the annealing at 800 K. The stabilization implies the building up of a new matrix incorporating the Co–O bond which requires the displacement of oxygen ions from the bulk MoO_3. In other words, the mixture of oxides detected at the surface, including the metal ions Mo^{6+}, Mo^{5+}, Mo^{4+} and Co^{2+}, transforms into the more stable $CoMoO_4$ compound with mainly Mo^{6+} and Co^{2+} metal ions.

More information may possibly be obtained by Co deposition at higher temperatures than those reported here. Experiments in this sense are ongoing.

4. Conclusions

The initially deposited Co atoms react at once with MoO_3 even at 90 K with formation of Co^{2+}, while Mo^{6+} is partially reduced to Mo^{5+} and Mo^{4+}. The contributions of all the species was determined by fitting procedures involving restrictions in peak position, peak FWHM, and spin orbit splitting. With increasing Co deposition, Co^0 becomes detectable on the topmost surface layer, especially at 90 K because of a restricted diffusion.

Annealing of the system at 800 K causes a 0.4 eV shift of the Mo^{6+} 3d signal towards a lower BE, with a simultaneous decrease of the contribution of Mo^{4+} and Mo^{5+} to the overall peak intensity. All the Co^0 species are oxidized to Co^{2+} during annealing and a shift of the Co^{2+} signal towards higher energies can be observed.

The valence band region shows clearly the changes that the substrate undergoes upon Co deposition: first, the formation of a conducting layer and the loss of conductivity on annealing.

The shape of the O 1s peak suffers a deformation towards higher BE as the amount of deposited Co increases. This is assigned to a distortion of the MoO_3 matrix by the incoming Co^{2+} ions, which implies some loss in crystallinity. This peak deformation is reversed by annealing, suggesting that a new ordered matrix has been built up incorporating the Co^{2+} ions.

The comparison with literature data leads to the conclusion that after the annealing procedure a Co molybdate is formed on the surface.

Acknowledgements

The authors are thankful for financial support to the following agencies: in Argentina, SeCyt (project 5.152-8/96) and CONICET (Argentine Research Council); in Germany, BMBF (project ARG 6L1A6A) and the Verband der Chemischen Industrie.

References

[1] M.T. Tatibouët, J.E. Germain, J. Catal. 76 (1982) 238.
[2] J. Ziólkowsky, J. Catal. 80 (1983) 263.
[3] A. Rahmouni, C. Barbier, J. Mol. Struct. 330 (1995) 359.
[4] H.F. Liu, R.S. Liu, D.J. Liew, R.E. Johnson, J.H. Lunsford, J. Am. Chem. Soc. 106 (1984) 4117.
[5] M.M. Kahn, G.A. Somorjai, J. Catal. 91 (1985) 263.
[6] N.D. Spencer, C.J. Pereira, R.K. Graselli, J. Catal. 126 (1990) 546.
[7] M.R. Smith, U.S. Ozkan, J. Catal. 141 (1993) 124.
[8] M.R. Smith, U.S. Ozkan, J. Catal. 142 (1993) 226.
[9] S. Pack, M.P. Rosynek, J.H. Lunsford, J. Phys. Chem. 98 (1994) 11786.
[10] J.-G. Choi, L.T. Thompson, Appl. Surf. Sci. 93 (1996) 143 and references therein.
[11] G. Mestl, B. Herzog, R. Schlögel, H. Knözinger, Langmuir 11 (1995) 3027.
[12] A. Michalak, K. Hermann, M. Witko, Surf. Sci. 366 (1996) 323.
[13] A. Papakondylis, P. Sautet, J. Phys. Chem. 100 (1996) 10681.
[14] C.V. Caceres, J.L. García Fierro, J. Lázaro, A. López Agudo, J. Soria, J. Catal. 122 (1990) 113.
[15] Y. Matsuoka, M. Niwa, Y. Murakami, J. Phys. Chem. 94 (1990) 1477.
[16] F.G. Requejo, A.G. Bibiloni, Langmuir 12 (1996) 51, and references therein.
[17] T.A. Patterson, J.C. Carver, D.E. Leyden, D.M. Hercules, J. Phys. Chem. 80 (1976) 1700.
[18] I. Alstrup, I. Chorkendorff, R. Candia, B.S. Clausen, H. Topsöe, J. Catal. 77 (1982) 397.
[19] N.S. McIntyre, D.D. Johnston, L.L. Coatsworth, R.D. Davidson, J.R. Brown, Surf. Interface Anal. 15 (1990) 265, and references therein.
[20] B. Klingenberg, F. Grellner, D. Borgmann, G. Wedler, Surf. Sci. 296 (1993) 374.
[21] F. Grellner, B. Klingenberg, D. Borgmann, G. Wedler, Surf. Sci. 312 (1994) 143.
[22] F. Grellner, B. Klingenberg, D. Borgmann, G. Wedler, J. Electron Spectrosc. Relat. Phenom. 71 (1995) 107.
[23] B. Klingenberg, F. Grellner, R. Haseneder, D. Borgmann, G. Wedler, Surf. Sci. 340 (1995) 153.
[24] B. Klingenberg, F. Grellner, D. Borgmann, G. Wedler, Surf. Sci. 383 (1997) 13.
[25] H. Wetzel, G. Meyer, D. Borgmann, G. Wedler, Chem.-Ing.-Tech. 63 (1991) 613.
[26] U. Kestel, G. Fröhlich, D. Borgmann, G. Wedler, Chem. Eng. Technol. 17 (1994) 390.
[27] G. Fröhlich, U. Kestel, J. £ojewska, T. £ojewski, G. Meyer, M. Voß, D. Borgmann, R. Dziembaj, G. Wedler, Appl. Catal. A: Gen. 134 (1996) 1.
[28] M. Voß, G. Fröhlich, D. Borgmann, G. Wedler, J. Catal. 187 (1999) 348.
[29] G. Benitez, J.L. Carelli, J.M. Heras, L. Viscido, Langmuir 12 (1996) 57.
[30] L.D. López-Carreño, G. Benítez, L. Viscido, J.M. Heras, F. Yubero, J.P. Espinós, A.R. González-Elipe, Surf. Interface Anal. 26 (1998) 235.
[31] L.D. López-Carreño, J.M. Heras, L. Viscido, Surf. Sci. 377–379 (1997) 615.
[32] R. Kleyna, H. Mex, M. Voß, D. Borgmann, L. Viscido, J.M. Heras, Surf. Sci. 433–435 (1999) 723.

[33] B. Brox, I. Olefjord, Surf. Interface Anal. 13 (1988) 3.
[34] V.M. Jiménez, A. Fernández, J.P. Espinós, A.R. González-Elipe, J. Electron Spectrosc. Relat. Phenom. 71 (1995) 61.
[35] K.S. Kim, Phys. Rev. B 11 (1975) 2177.
[36] M.O'Keeffe, Fast Ion Transport in Solids, North-Holland, Amsterdam, 1973, p. 233.
[37] J.C. Fuggle, E. Umbach, R. Kakosche, D. Menzel, J. Electron Spectrosc. Relat. Phenom. 26 (1982) 111.
[38] P.S. Bagus, Ch.W. Bauschlicher, J. Electron Spectrosc. Relat. Phenom. 20 (1980) 183.
[39] L. Khilborg, Ark. Kemi 21 (1963) 357.